94-GT-2

LEADING EDGE FILM COOLING OF A TURBINE BLADE MODEL THROUGH SINGLE AND DOUBLE ROW INJECTION: EFFECTS OF COOLANT DENSITY

M. Salcudean, I. Gartshore, K. Zhang, and Y. Barnea
Department of Mechanical Engineering
University of British Columbia
Vancouver, British Columbia, Canada

BREAK

ABSTRACT

Experiments have been conducted on a large model of a turbine blade. Attention has been focussed on the leading edge region, which has a semi-circular shape and four rows of film cooling holes positioned symmetrically about the stagnation line. The cooling holes were oriented in a spanwise direction with an inclination of 30° to the surface, and had streamwise locations of ±15° and ±44° from the stagnation line. Film cooling effectiveness was measured using a heat/mass analogy. Single row cooling from the holes at 15° and 44° showed similar patterns: spanwise averaged effectiveness which rises from zero at zero coolant mass flow to a maximum value $\overline{\eta}^*$ at some value of mass flow ratio M^*, then drops to low values of $\overline{\eta}$ at higher M. The trends can be quantitatively explained from simple momentum considerations for either air or CO_2 as the coolant gas. Close to the holes, air provides higher $\overline{\eta}$ values for small M. At higher M, particularly farther downstream, the CO_2 may be superior. The use of an appropriately defined momentum ratio G collapses the data from both holes using either CO_2 or air as coolant onto a single curve. For $\overline{\eta}^*$, the value of G for all data is about 0.1. Double row cooling with air as coolant shows that the relative stagger of the two rows is an important parameter. Holes in line with each other in successive rows can provide improvements in spanwise averaged film cooling effectiveness of as much as 100% over the common staggered arrangement. This improvement is due to the interaction between coolant from rows one and two, which tends to provide complete coverage of the downstream surface when the rows are placed correctly with respect to each other.

NOMENCLATURE

Symbols

d - hole cross-sectional diameter

C_p - pressure coefficient, $\dfrac{p - p_\infty}{\frac{1}{2}\rho_\infty U_\infty^2}$

C - concentration of contaminant

G - momentum flux ratio $\dfrac{\rho_c U_c^2}{\left(\rho_\infty U_I^2\right)} = \dfrac{M^2}{R(1 - C_p)}$

G^* - value of G at which maximum $\overline{\eta}$ occurs

M - mass flux ratio, $\dfrac{\rho_c U_c}{\rho_\infty U_\infty}$

M^* - value of M at which maximum $\overline{\eta}$ occurs

M_∞ - value of M averaged over all coolant holes for double row cooling

p - static pressure measured at a streamwise position on the model

R - coolant-to-gas density ratio, ρ_c/ρ_∞

Re - Reynolds number $U_c\ d/\upsilon_c$

S - spanwise spacing between holes in one row ($S/d = 4$ in all rows at all times in the present experiments)

S_R - relative spanwise spacing between the holes in successive rows; $S_R = 0$ is fully staggered; $S_R/d = 2$ is fully in line in this experiment.

T - temperature

U_c - average coolant velocity from all open holes

U_∞ - flow velocity far from the model

U_l - velocity of fluid just upstream of coolant holes but outside boundary layers

x - curved streamwise distance measured from stagnation line

z - spanwise distance

η - film cooling effectiveness, $\dfrac{T_{AW} - T_\infty}{T_c - T_\infty}$ or $\dfrac{C_w}{C_c}$ in the present experiments

$\overline{\eta}$ - spanwise averaged film cooling effectiveness (averaged over spanwise interval of S)

$\overline{\eta}^*$ - maximum value of $\overline{\eta}$ at one value of x/d

ρ - density

θ - angle around semi-circular leading edge, measured from stagnation line

υ - kinematic viscosity

Subscripts

∞ - free stream, upstream of model

15 - referring to holes at $\theta = 15°$

44 - referring to holes at $\theta = 44°$

c - coolant

w - at wall

AW - for an adiabatic wall

1. INTRODUCTION

Film cooling is a method of protecting turbine blades and other surfaces from the harsh environment of a very hot free stream fluid downstream of combustion. For turbine blades, previous work has shown that the stagnation region near the leading edge is a particularly critical region since it suffers such intense exposure to the hot free stream, and that this region needs investigation with particular emphasis on the cooling effect very close to the holes. In addition, the curvature of the surface and the fluid mechanics of injection both suggest that a significant component of spanwise injection is important. The curvature of the surface dictates that if the coolant injection angle relative to the surface is to be small, as is desirable to avoid separation at reasonable mass flow rates, then the hole must be directed in a spanwise or partly spanwise direction to avoid complicated hole curvatures and intersections. In addition, the use of spanwise injection allows a larger spanwise region to be covered from one hole than would be possible with stream-wise injection. This allows the holes to be placed farther apart and makes the physical arrangements simpler for effective downstream cooling. Therefore, this report concentrates on leading edge region film cooling with single and double rows of holes oriented to produce spanwise blowing close to the stagnation line. The report is largely experimental, but an attempt will be made to explain the results using simple physical arguments.

Two fluids, air and CO_2, are used alternatively as the coolant to simulate the effects of changing density. The coolant is typically at higher density than the free stream in practice, and the use of CO_2 goes some way toward showing the effect of this parameter on the resultant downstream film cooling. The results concentrate on the region very close to the holes in one row or two rows since, in the leading edge region, the near hole region is even more important than would be the case farther downstream. By using the heat/mass analogy, a precisely adiabatic wall is maintained. The film cooling effectiveness, characteristic of one aspect of film cooling modeling, is measured. The use of this film cooling effectiveness and its complementary quantity, the heat transfer coefficient based on the adiabatic temperature at the wall, have been well covered in previous literature and will not be reviewed here (Eckert, 1984).

The objectives of this paper are: 1) to investigate the effectiveness of a single row of coolant holes providing purely spanwise injection, first with air as the coolant and then with CO_2, and 2) to investigate the interaction between two rows of coolant holes and, in particular, to observe the effect of varying the spanwise relative spacing of the holes in successive rows.

2. REVIEW OF LITERATURE

The concept of film cooling for the protection of surfaces and, in particular, the protection of turbine blades is not new. An excellent paper by Luckey et al. (1977), describes gas film cooling for turbine blades in the leading edge stagnation region and reports heat transfer measurements expressed as spanwise averaged Stanton numbers for various mass flow ratios (M), at one particular density ratio (R), for holes at 20°, 30° and 40° from the stagnation line of a circular cylinder. These results show a reduction in Stanton number with increasing mass flow ratio (M) until a minimum is reached near a mass flow ratio of 1, followed by a decrease in the effectiveness of cooling for higher mass flow ratios. Thus, the film cooling starts from zero at zero coolant mass flow, rises to a maximum at about $M = 1$, and then decreases due to the mixing and separation effects which arise from high momentum in the coolant. The data and discussion center around spanwise injection from the cooling holes with spanwise averaged Stanton number plotted both as a function of hole position and as a function of mass flow ratio. More recent papers include that of Karni and Goldstein (1990), in which the authors simulate heat transfer from a circular cylinder in cross flow using a mass transfer naphthalene sublimation technique. They conclude, very reasonably, that the injection position relative to the stagnation line is extremely important. They investigate both streamwise and spanwise injection, showing that the efficiency of film cooling decreases downstream and decreases at high mass flow ratios.

Another recent paper by Nirmalan and Hilton (1990) describes film cooling from holes near the leading edge of a turbine blade model. These authors conclude that film

cooling can be very effective for some distance downstream, that the static pressure measured over the blade is largely unaffected by blowing over the range of mass flow ratios investigated and that the downstream film cooling is a complicated function of two competing mechanisms: 1) the thermal dilution due to the injection of relatively cold fluid decreasing heat transfer to the blade, and 2) turbulence augmentation due to the injection process increasing heat transfer. It is helpful to have these physical mechanisms clearly identified and an attempt will be made to follow this direction in the present paper.

Mehendale and Han (1992) describe the effects of free stream turbulence on leading edge film cooling. Two rows of holes at θ = 15° and 40° were used with spanwise blowing and spanwise spacing S/d = 3. Freestream turbulence slightly reduced the spanwise averaged film cooling effectiveness $\overline{\eta}$ just downstream of the second row of holes for low blowing rates (M_∞ = 0.4), but slightly increased this $\overline{\eta}$ for higher blowing rates (M_∞ = 0.8). A progressive decrease in $\overline{\eta}$ at this location is found with increasing M_∞, the largest changes occurring at low turbulence levels. These results suggest that free stream turbulence increases mixing so that $\overline{\eta}$ is reduced at low M_∞, where separation is not significant but lowers separation effects and thereby raises $\overline{\eta}$ at larger values of M where $\overline{\eta}$ has already been significantly reduced by separation effects.

More recent papers include computational studies of film cooling of turbine blades, and two will be mentioned here. Garg and Gaugler (1993) use a three-dimensional Navier-Stokes code and a general body-fitted coordinate system. A power law representation for the hole exit velocity profile was used. Experimentally measured wall temperatures were specified as boundary conditions and wall heat flux was calculated. An excellent paper by Leylek and Zerkle (1993) provides a three-dimensional elliptic Navier-Stokes solution for inclined holes in a flat plate, not in a stagnation region. Their solutions include internal and external regions, and their conclusions are clear and important. In particular, they draw attention to the effect of the length of the hole connecting the film cooling plenum to the film hole exit. Their conclusions are that, for a hole length of about 4 times the hole diameter (typical of actual turbine blades), there is a large separation region in the film cooling tube (for streamwise injection) which leads to surprising re-distributions of the coolant flow at the hole exit. This low l/d effect, which is probably present in actual turbine blade film cooling, must have an important influence on the downstream effectiveness. The present experimental arrangements use a hole length l/d of four, but the spanwise blowing of the present study adds further complications to the effects described by Leylek and Zerkle.

The importance of spanwise blowing and the fluid mechanics of its contribution to the film cooling of flat plates, was the subject of a recent computational paper by

Zhou et al. (1993). The calculated results show clearly why spanwise blowing gives rise to better coverage of the blade surface downstream of the coolant holes than does streamwise blowing.

3. EXPERIMENTAL ARRANGEMENTS

The experimental arrangements used for the present paper follow those described by Salcudean et al. (1994). These will be summarized here for convenience, but details are available in the previous publication.

Experiments were conducted in a large wind tunnel 2.4 m wide and 1.7 m high. The model has a semicircular leading edge diameter of 127 mm, parallel top and bottom lengths of 1.2 m, and an overall chordwise length of 2.3 m. Since the model spans the tunnel at zero incidence, the frontal blockage created by the model is simply the ratio of the model leading edge diameter to the tunnel height, about 8 percent. Notice that this differs from comparable studies done by others, such as Mick and Mayle (1988), in which the blockage ratio was 33 percent. Changes in blockage ratio change the pressure distribution over the model, and therefore change the ratio of flow rates coming from rows of holes located at different streamwise locations if all rows are fed from a common plenum (see comments in Salcudean et al. (1994)).

In the present experiments, either air or CO_2 was injected through coolant holes located in the front of the interior plenum. The coolant was regulated and metered before being ejected so that its density was known. Coolant holes were located at ±15° and ±44° from the stagnation line, as shown in Figure 1. The overall arrangement of the model in the wind tunnel and the arrangement of the removable plenum is shown in Figure 2. The holes in a row were located 4 hole diameters apart, and spanwise averages discussed later were taken over this spanwise length of 4 hole diameters. Each row consisted of 7 holes, and measurements covered the 3 holes at the spanwise centre of the row. Perfect symmetry of the holes about the stagnation line was always maintained. All cooling holes were 12.7 mm in diameter and were drilled with an inclination of 30° to a spanwise line on the cylindrical leading edge. This provides spanwise cooling with no streamwise component to the coolant holes. A small contamination of propane was mixed thoroughly with the coolant gas (either air or CO_2), and film cooling effectiveness was measured by sampling gas at the wall downstream of the coolant holes. The sampling was done through a specially designed rake of 13 very fine tubes (0.5 mm outside diameter) designed to lie directly on the wall. Gas sampled through these tubes was sent through suitable wafer switches to a flame ionization detector, which accurately measured the mean propane concentration. Suitable calibrations were done, both for air and CO_2 as coolant gas. Details can be found in Gartshore et al. (1993). Using the mass/heat analogy the film cooling effectiveness can be found directly from the concentration

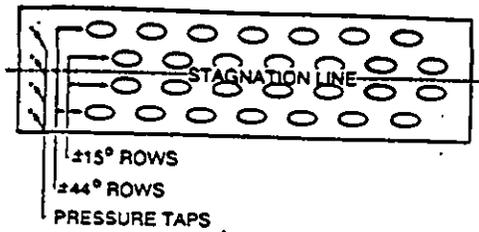of propane at the wall, and is $\dfrac{C_w}{C_c}$. Following preliminary
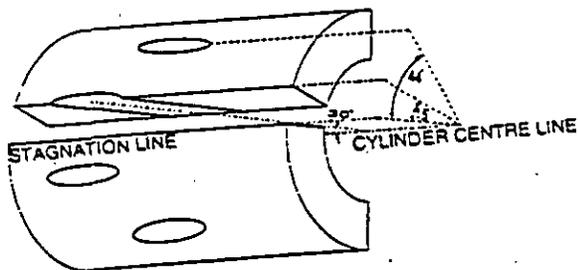
Figure 1a: Injection hole geometry.

±15° ROWS
±44° ROWS
PRESSURE TAPS

STAGNATION LINE
CYLINDER CENTRE LINE

Figure 1b: Leading edge hole pattern.

FENCES
PIVOT BARS
GUY WIRES

Figure 2a: Model turbine blade in test section.

SEMI-CIRCULAR LEADING EDGE
PERFORATED PLATE
SCREENS
FLOW BAFFLE
INLET

Figure 2b: Plenum schematic.

investigation, the use of tubes with a finite diameter to sample the propane concentration at the wall was found to have little error, and no corrections were made for the small offset from the wall, nor for the small suction disturbance created by the sampling process. Reynolds numbers of the coolant gas, (Re_c), were usually maintained at about 4000. In some cases lower values were required, but the value was never below 1000 for single row testing. The Reynolds number of the front row coolant flow necessarily drops to very low values for double row testing when the fluid flow from the front row approaches zero. To measure the distribution of cooling effectiveness over the surface, the rake is drawn gradually back over the surface, sampling from each tube at each streamwise location to provide a matrix of measurements from which detailed contours can be produced, and spanwise averages calculated. For air, R = 1; for CO_2, $R \approx 1.53$.

4. RESULTS AND DISCUSSION

4.1 Single Row Cooling
Before proceeding to describe the results obtained from the present measurements, it is worthwhile to review the effects expected for film cooling effectiveness just downstream of a row of holes placed near the stagnation point of a circular cylinder. In general, the spanwise average would be expected to be a useful measure of the film cooling effectiveness, and we will discuss what might be expected of this spanwise average as measured at a position just downstream of a row of film cooling holes as the mass flow of coolant is increased. The mass flow ratio,
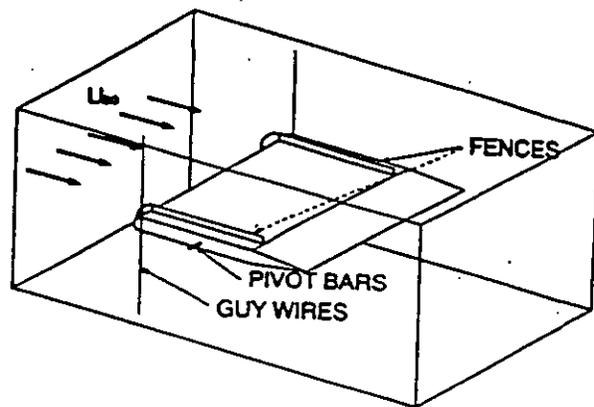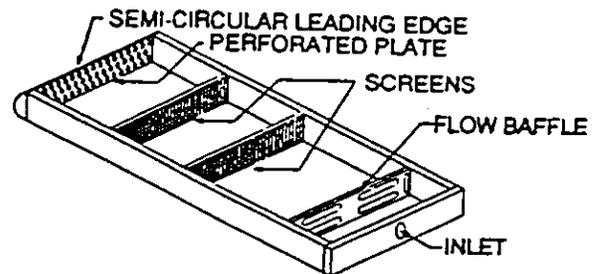
M, is defined in the usual way as $\dfrac{\rho_c U_c}{\rho_\infty U_\infty}$ (see nomenclature), and can be designated as M_{15} when referring to the mass flow from the holes at 15°, or as M_{44} when designating mass flow from the holes at 44°. When coolant flows from both rows, the average mass flow ratio, M_∞, is defined from the total coolant mass flow rate divided by the total cross-sectional coolant hole area so that

$$M_\infty = (M_{15} + M_{44})/2.$$

The spanwise averaged film cooling effectiveness for one row of holes will be zero at $M = 0$ and will increase as M increases due to the presence of the coolant downstream of the holes. The effectiveness will continue to increase until the tendency towards separation resulting from the coolant injection decreases the film cooling. The maximum spanwise averaged film cooling effectiveness will be reached at some particular value of M. Let us designate the maximum value of $\overline{\eta}$ as $\overline{\eta}^*$, and the value of M at which this maximum value occurs as M^*. The present notation
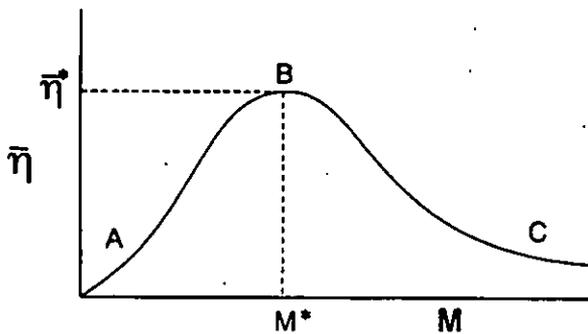
4

Figure 3: Trends of film cooling effectiveness
downstream of cooling holes.

Figure 4: Spanwise averaged effectiveness at X/d=2.5
for a single row of coolant holes located at 15°

follows the suggestions of Luckey et al. (1977). Referring to Figure 3, we can identify three regions designated as A, B, and C . At low values of M, there is too little coolant and too little spanwise momentum (using spanwise injection) to provide good coverage. At Region B, the optimum is reached, but there is increasing momentum from the coolant, and the coolant fluid starts to separate, to penetrate through the boundary layer, eventually mixing too much with the surrounding hot gas. Finally, at Region C, where the film cooling effectiveness is much reduced at high mass-flow ratios, there is considerable separation, considerable mixing, and inefficiency of the process.

First, let us consider the effect of the streamwise placement of holes. In the present experiments there are two rows of holes, one at 15° and one at 44°, measured from the stagnation line. These could be considered as typical of holes located close to and farther from stagnation. For holes at 15° in the present experiment, the static pressure, compared to the free stream static pressure, will be relatively high since the hole is located close to the stagnation line. The hole at 44° will have a lower static pressure, so that the flow coolant rate out of the 15° hole will always be less than that out of the 44° hole if both of the hole rows having the same geometry are fed from a common plenum. This effect has been described quantitatively by Gartshore et al. (1993) and Salcudean et al. (1994).

A second important effect of the free stream is that the cross stream velocity approaching the 15° hole will be considerably lower than the cross stream velocity approaching the 44° hole. The cross stream velocity in the free stream outside the boundary layer just upstream of the holes is, of course, connected to the static pressure through Bernoulli's equation, but it is the cross stream velocity approaching the hole compared to the average velocity out of the hole (the coolant velocity) which determines the kinematic flow pattern near the hole. The ratio of approach velocity U_I to coolant velocity U_c is therefore very important and will be explicitly accounted for later in this paper.
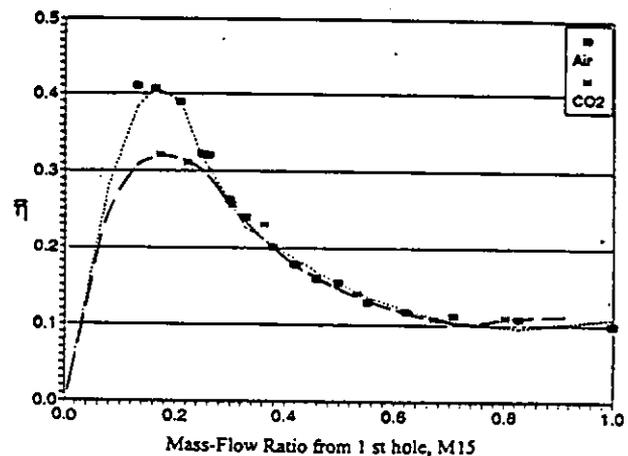
A third difference between the two holes is that although there is a favourable (negative) pressure gradient over the 15° hole, this is fairly small in comparison with the favourable gradient over the 44° hole. The gradient over the 44° hole is close to the maximum possible on the semi-circular leading edge of this model. Despite the favourable pressure gradients which exist over the semi-circular leading edge, it is likely that the boundary layer thickness approaching the second hole at 44° will be larger than the boundary layer thickness approaching the first hole at 15°, and this will be particularly true if there is blowing from the 15° set of holes. Blowing at low or moderate mass flow ratios is likely to reduce the momentum close to the wall and increase the effective boundary layer thickness approaching the second set of holes.

Let us now turn to the actual results from the present experiment. Figure 4 shows the spanwise averaged film cooling effectiveness at $x/d = 2.5$, which is 1.19 hole diameters downstream of the first row centreline of holes at 15°. Only that row is open. Plotted against the mass flow ratio M_{15} for that one row is the spanwise averaged film cooling effectiveness $\overline{\eta}$. This figure shows that there is a maximum $\overline{\eta}$ reached for both air and CO_2, as anticipated in the previous discussion and in Figure 3. The values at low mass flow ratios are not well defined, but the peak is fairly clear, and the peak value M_{15}^* in the present notation occurs for air at about 0.16 and for CO_2 at about 0.2. M_{15}^* for CO_2 is, therefore, higher than that for air. This difference occurs because the peak value of the film cooling effectiveness is determined largely by momentum rather than by mass. If one calculates a local hole momentum flux ratio defined as $\dfrac{U_c^2 \rho_c}{U_\infty^2 \rho_\infty}$ this is equal to $M^2 \rho_\infty/\rho_c$. Calculating the momentum flux ratio for air and that for CO_2 at the peak, one finds from the present numbers
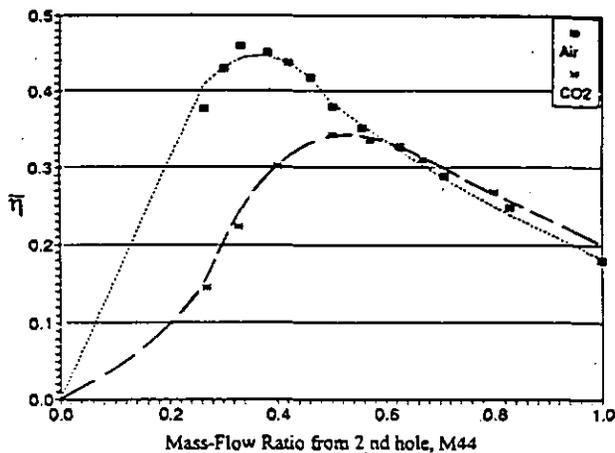
5

Figure 5: Spanwise averaged effectiveness at X/d=5.0
for a single row of coolant holes located at 44°

Figure 6: Spanwise averaged effectiveness at X/d=10
for a single row of coolant holes located at 44°

already noted that they are roughly equal at the peak values. There is no great accuracy in this calculation, but it is reassuring to find that the momentum flux at the peak is roughly the same for both air and CO_2 as would be intuitively expected.

Figure 5 presents the results for the second row of holes at 44° only, and plots the film cooling effectiveness at $x/d = 5$, 1.16 hole diameters downstream of the centreline of that row of holes against the mass flow ratio. From this figure, we see that $M_{44}^{\bullet}$, the value of mass flow ratio for the maximum film cooling effectiveness, is about 0.35 for air and about 0.55 for CO_2, again showing the trend that the maximum occurs at a higher value of M for CO_2 than for air. In this case, a similar calculation of the momentum ratio shows that the agreement between values calculated for air and CO_2 is not as good as was the case for the first set of holes at 15°, but it is reassuring that the same trends are evident.

By comparing the value of $M^{\bullet}$ in Figure 4 with the value of $M^{\bullet}$ in Figure 5, it can be seen that the peak film cooling effectiveness occurs at a much lower mass flow ratio for the first row of holes in Figure 4 than it does in Figure 5 for the second row of holes. This is because the velocities in the flow outside the boundary layer, just upstream of the holes is very much larger for the second row of holes than for the first. This can be quantified by calculating the value of the average coolant velocity (U_c) divided by the local velocity just upstream of the holes (U_l). This local velocity, upstream of the holes, can be found from the pressure coefficient measured near the hole at the same position. This pressure coefficient (C_p), defined in the usual way, is

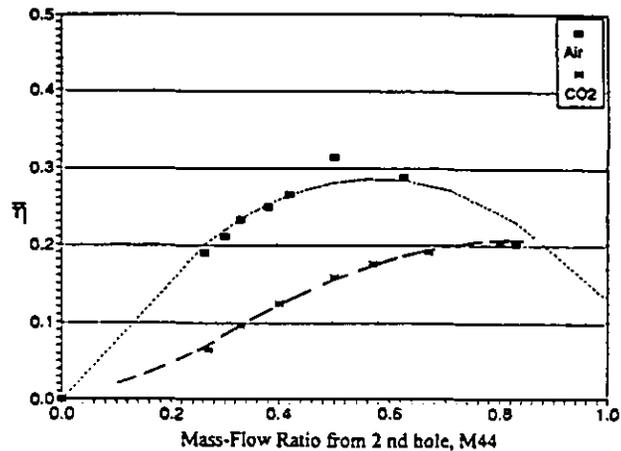equal to $\left(1 - \dfrac{U_l^2}{U_\infty^2}\right)$ at low Mach number and is about 0.75

for the holes at 15° and about -0.5 for the holes at 44°. From these, the velocities just upstream of the holes can be

calculated. The ratio $\dfrac{U_c}{U_l}$ is equal to $\dfrac{M}{\sqrt{1-C_p}}\dfrac{\rho_\infty}{\rho_c}$ which

is about 0.3 at maximum η for the air coolant for both the holes at 15° and the holes at 44°. Thus, the peak occurs when the ratio of the coolant velocity to the local velocity just upstream of the holes is approximately the same value regardless of the hole position. Some variation in these values can be expected because of boundary layer effects, but again it is reassuring to see that the trends in the present data can be rationalized both qualitatively and quantitatively. Very similar trends can be observed from Figures 4 and 5 for the CO_2 coolant injection. $M^{\bullet}$ in Figure 4 is about 0.20 for CO_2 injected at 15° and about 0.55 for CO_2 injected at 44°. In both of these cases the

values of $\dfrac{U_c}{U_l}$ are between 0.25 and 0.30 for the two sets

of holes when CO_2 is used as the coolant. Taking the lower

value of 0.25 for the peak value of $\dfrac{U_c}{U_l}$ for CO_2 coolant, the

momentum ratio $\rho_c U_c^2 / \left(\rho_\infty U_l^2\right)$, which occurs at the peak film cooling effectiveness, is essentially the same for both air and CO_2 coolant cases, as expected. This definition of momentum ratio combines effects of density and hole position in a single ratio. It describes the appropriate non-dimensional momentum flux at $M^{\bullet}$ for the present geometry.

Another observation which can be made from Figures 4 and 5 is that the value of maximum film cooling effectiveness $\overline{\eta}^{\bullet}$ is higher for air than it is for CO_2. In Figure 4 we see that $\overline{\eta}^{\bullet}$ for air is about 0.4, whereas it is
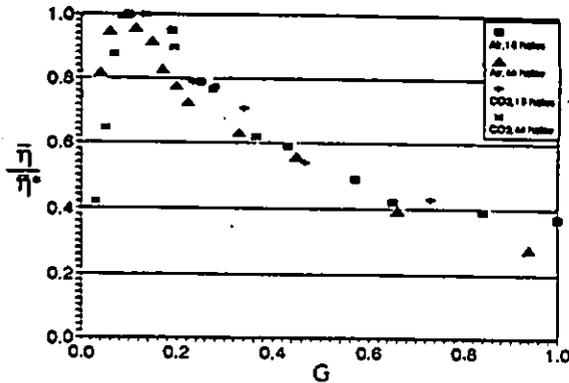
6

Figure 7: Spanwise averaged effectiveness data replotted in terms of momentum ratio.

about 0.30 for CO_2 for holes at 15°. A similar trend is observed in Figure 5 for the holes at 44° where $\overline{\eta}^*$ is 0.45 for air and 0.35 for CO_2. The differences in effectiveness for the two kinds of coolant must be attributed to differences in the volume flow rate of the coolant, which is considerably lower for CO_2, and to differences in the mixing between the denser CO_2 and surrounding air in comparison with the mixing which occurs when air is the coolant. No quantitative estimate of the differences can be made at this time, but it is worth noting that the local maximum effectiveness of a dense coolant is less than that of a coolant which has the same density as the free stream gas in these experiments at least at low M. This is similar to results obtained by Ou and Han (1993) from a model turbine blade cascade. However, Pedersen et al. (1977) report $\overline{\eta}$ values close to a row of closely spaced coolant holes providing streamwise injection on a flat plate, and show that maximum values of $\overline{\eta}$ actually increase with increasing R. Both lateral hole spacing and hole orientation must be significant factors in this trend, and further work is required to determine the effects of these variables.

Figure 6 shows the spanwise averaged film cooling effectiveness plotted at $x/d = 10$ farther downstream of the second row of holes when only the second row is operating. This shows how the film cooling effectiveness changes with downstream distance x/d. As expected, the maximum film cooling drops because of the increased mixing which occurs between $x/d=5$ and $x/d = 10$. The maximum $\overline{\eta}^*$ in Figure 6 for air is something like 0.3, whereas it is about 0.45 at $x/d = 5$. A similar trend occurs for CO_2 although for $x/d = 10$ and CO_2 as the coolant, there is no clear maximum observed in the data gathered in this experiment. Based on the somewhat limited data presented in Figure 6, and comparable data in Figure 5, it is clear that the value of M^* increases with increasing distance from the hole. The shapes of these curves suggest that the film cooling effectiveness with CO_2 as the coolant will surpass that with air as the coolant, particularly at higher mass flow ratios, far downstream from the holes. This is in agreement with the results described by Gartshore et al. (1993) which

showed that far downstream of the holes, CO_2 provided a better spanwise averaged film cooling effectiveness, but that close to the holes the spanwise averaged film cooling effectiveness was greater for air than for CO_2.

Based on the use of a momentum ratio $\rho_c U_c^2 / (\rho_\infty U_l^2)$, which we denote here by G, much of the data just downstream of a single row of holes located anywhere using any coolant fluid should collapse onto a single curve. The momentum ratio G can be rewritten in terms of pressure coefficient C_p, the density ratio R and the mass flow ratio as follows:

$$G = \rho_c U_c^2 / \rho_\infty U_l^2$$

$$= \left(\frac{\rho_c U_c}{\rho_\infty U_\infty}\right)^2 \frac{U_\infty^2}{U_l^2} \frac{\rho_\infty}{\rho_c}$$

$$= M^2 / [(1 - C_p)R]$$

The use of G is explored in Figure 7 where data from the four cases described in Figures 4 and 5 are replotted as $\overline{\eta}/\overline{\eta}^*$ versus momentum ratio G. Although there is some scatter, the collapse achieved when all data is plotted in this way strongly supports the use of a momentum ratio as far as maximum effectiveness and high mass flow ratios are concerned. At low M it is likely that mass flow ratio M is an increasingly important parameter by itself, and in general it must be expected that both M and G play some role, particularly below M^*. However, for the present spanwise injection geometry with $s/d = 4$, the value of the momentum ratio G^* which provides the maximum spanwise averaged effectiveness is close to 0.1. This appears to be valid for a range of hole positions and coolant fluids. As the stagnation line is approached, θ becomes small, C_p approaches unity, and $\overline{\eta}^*$ will occur at very small values of M. When the row of holes injects fluid on both sides of a stagnation line, which will occur when θ becomes small enough, the present conclusions are no longer valid.

Note also that the data collapse in Figure 7 is possible only when data are taken equally close to both sets of holes. The present data were taken 1.19 d behind the upstream hole centreline (at 15°) and 1.16 d behind the downstream hole centreline (at 44°). If these distances were not fairly small and very nearly equal, the collapse of data would not be as good.

The general picture that emerges is in agreement with the anticipated sketch of Figure 3, in that the spanwise averaged cooling effectiveness rises from zero, at zero mass flow rates, to a maximum $\overline{\eta}^*$ occurring at a mass flow ratio M^*, and then drops off. The values of $\overline{\eta}^*$ are higher
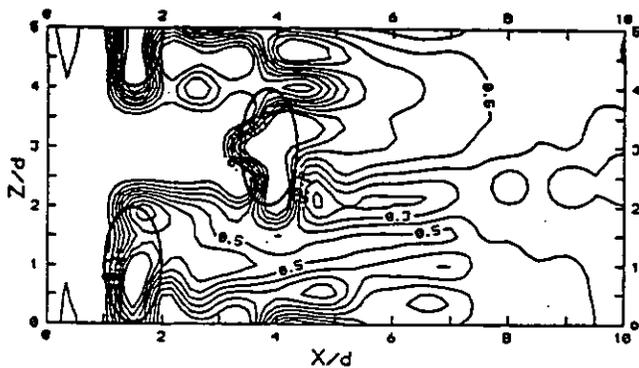
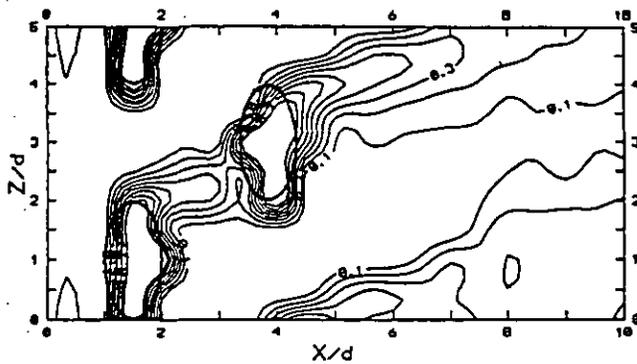Figure 8a : Iso-effectiveness contours for $M_\infty= 0.52$, Re ≈ 4200 and air as coolant. $Sr/d=0$.

Figure 8b: Iso-effectiveness contours for $M = 1.19$, Re ≈ 4200 and air as coolant. $Sr/d=0$.

for air than for CO_2, whereas the value of M^* is lower for air than for CO_2. Very close to the hole, and this is true for either the holes at 15° or 44°, it appears that air as the coolant will be superior to CO_2 only at low M. Use of a momentum ratio G collapses much of the data satisfactorily and Figure 7 shows that G^* is approximately 0.1.

4.2 Double Row Cooling

For the reasons already described, the spanwise averaged film cooling effectiveness just downstream of a double row of holes will have trends like those of Figure 3. Very low values of M_∞ cannot be investigated in the double row coolant injection since free stream fluid goes *into* the front row of coolant holes if the value of M_∞ is too low because of the high static pressure there. Hence, Region A of Figure 3 may not be evident for double row cooling, but the pattern of a particular value of mass flow ratio M_∞^* at which a maximum value of $\overline{\eta}$ is reached is still useful. Again, as for single row coolant injection, M_∞^* will be lower for air than for CO_2, and $\overline{\eta}^*$ will be lower for CO_2 than for air, at least when measurements are made close to the holes. As observed by Gartshore et al. (1993), it is likely that CO_2 will provide superior effectiveness at large M_∞ while air provides superior $\overline{\eta}$ at low M_∞. Effects

are now complicated by the interaction of the coolant from the two rows, and simple momentum arguments, plausible for single rows, are no longer easy to apply.

This section describes results obtained when coolant air (not CO_2) was ejected simultaneously through both the 15° and the 44° rows from a common plenum. Previous results have shown that the flow from the first row of holes, under certain conditions of mass flow rate, is directed at the holes in the second row. In Figure 8 of this paper (repeated from Gartshore et al. (1993)), we see the iso-effectiveness contour lines for mass flow ratios of 0.52 and 1.19 when air is used as coolant. For the first mass flow ratio (0.52), there is a broad coverage of the surface downstream of the second set of holes, whereas, for a mass flow ratio of 1.19 there are large areas of the surface not covered by coolant. Part of the reason for the failure at high mass flow ratios is the separation and mixing caused by large injection velocities, but part of the problem is also due to the fact that the coolant from the first row of holes is directed by its spanwise momentum toward the holes of the second row. As noted in earlier reports, the relative placement of the holes in the second row determines the degree of this interaction (see Mick and Mayle (1988), Gartshore et al. (1993), and Salcudean et al. (1994)).

In order to investigate the importance of this effect, measurements were made with the present model in which the first row of holes was displaced in the Z direction by various amounts, thereby changing the hole pattern from one which is fully staggered to one which can be fully in line. At any one mass flow ratio there is an optimum value of the relative position of the two rows of holes which will produce the highest spanwise averaged film cooling effectiveness just downstream of the second row. We define S_R as the distance that the first row of holes (those at 15°) is displaced in the Z direction from its original, fully staggered position. In this notation, $S_R/d = 0$ will denote the fully staggered arrangement already described; $S_R/d = 2$ will denote a fully in-line pattern, and $S_R/d = 4$ will provide a fully staggered position identical to that for $S_R/d = 0$. Figure 9 shows the spanwise averaged film cooling effectiveness just downstream of the second row of holes, i.e., at $x/d = 5$ as a function of the displacement of the first row (S_R/d) for various mass flow ratios. The mass flow ratios, M_∞ , in this case are the average value taken as the total coolant mass flow divided by the total hole area of all rows of holes.

It is clear that at lower mass flow ratios (0.52 and 0.64), the initial effect of increasing S_R/d is to decrease the spanwise averaged effectiveness. This is not surprising in view of the contours of Figure 8 which show that a fairly good coverage is obtained at low mass flow ratios from the two sets of holes. At higher mass flow ratios such as $M_\infty = 1.19$, improvements are noted with small displacements of S_R/d. Again, this is not surprising considering the rather unfortunate interaction shown for large mass flow ratios in the contour lines of Figure 8. The surprising result
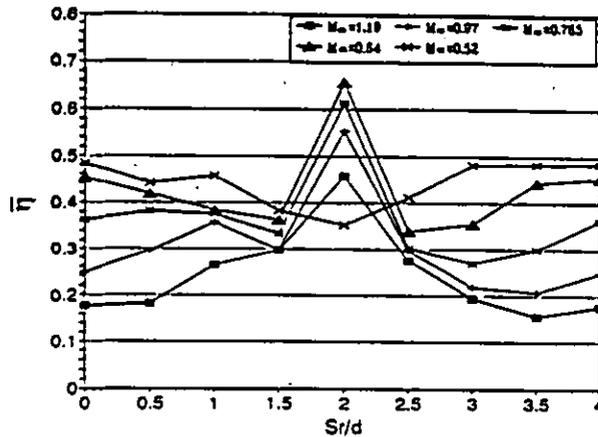
Figure 9 : Effects of relative stagger between two rows of coolant holes at various overall mass flow ratios. Measurements of $\bar{\eta}$ were at $x/d=5$.
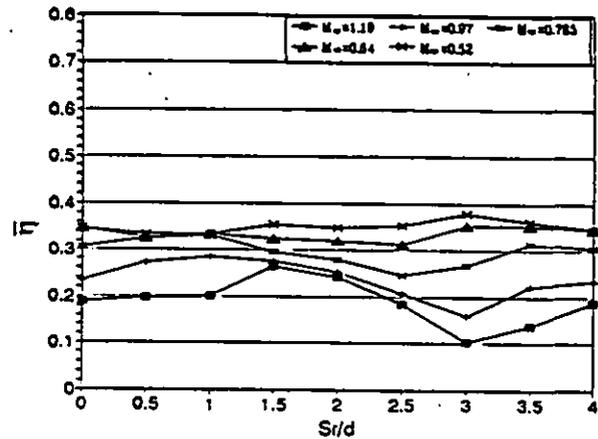

Figure 10 : Effects of relative stagger between two rows of coolant holes at various overall mass flow ratios. Measurements of $\bar{\eta}$ were at $x/d=10$.

shown in Figure 9 is that, for in-line holes, i.e., for $S_R/d = 2$, quite high spanwise averaged film cooling effectiveness values are obtained for a wide variety of mass flow rates, suggesting that the staggered pattern, which is common in film cooling arrangements, is by no means the best pattern.

The improvements in spanwise averaged film cooling effectiveness found by changing the relative stagger can be quite dramatic, extending to as much as a factor of 2 when the holes are in line, compared to the case when the holes are fully staggered. Clearly these results will change with geometry and would, of course, change if the holes in the two rows were located at different spanwise spacings or streamwise positions, or if each row of holes had its own separate plenum. The optimum shift position, i.e., the best value of S_R/d, will clearly depend upon the coolant as well, and could be expected to change if CO_2 or a denser gas were used for the coolant injection. The present results are not surprising since the trends were anticipated by several authors, but the degree of improvement which can be obtained by moving a row laterally is surprisingly large.

Figure 10 shows the effects of this spanwise movement of the first row of holes on the spanwise averaged film cooling effectiveness at $x/d = 10$ some distance downstream of the two rows of holes. The effects of the spanwise movement S_R/d at this larger streamwise position are less dramatic than those shown in Figure 9 so that the spanwise relative displacement of the rows is an effective optimization near the holes and is less important farther downstream, as expected. The effects of having holes in line would have to be assessed as far as the structural integrity of the blade and internal cooling is concerned, but from the present results, it appears that an arrangement other than the simple staggered one is certainly worth considering for film cooling applications near the leading edge where the near hole region is particularly important.

5. CONCLUDING DISCUSSION

For the leading edge region of the blade model, attention has been focussed on streamwise positions very close to the coolant holes. The immediate neighborhood of the holes is important near the leading edge since this region is subjected to such intense thermal effects. Spanwise averaged film cooling effectiveness has been used as a simple description of the film cooling at each streamwise position. While this average disguises the details of the η spanwise distribution, it allows a single measure of effectiveness of each x to be used in simple arguments to explain the observed trends. The present experiments using spanwise injection of coolant from a single row of holes show that the spanwise averaged film cooling effectiveness just downstream of the row reaches a maximum value which is strongly dependent on the hole downstream position and on the coolant density. This sensitivity is a result of differences in the velocity of the oncoming fluid just upstream of the hole. The effect can be estimated by using simple arguments, and shows that the ratio of U_c to U_1 at maximum effectiveness is about 0.3 for air and slightly less for CO_2. Clearly the mass flow ratio which should be used to provide this optimum film cooling effectiveness varies dramatically with the hole position, since the oncoming fluid velocity is also a strong function of the hole position. In addition, the value of mass flow ratio necessary to provide the maximum spanwise averaged film cooling effectiveness depends upon the fluid density used for the coolant, and is higher for a denser fluid than when air is used as the coolant fluid. A single momentum flux ratio describing the coolant momentum as a fraction of the fluid momentum just upstream of the holes, identifies the conditions under which spanwise averaged film cooling effectiveness reaches a maximum, and collapses much of the present data for film cooling from a single row of holes at any downstream position.
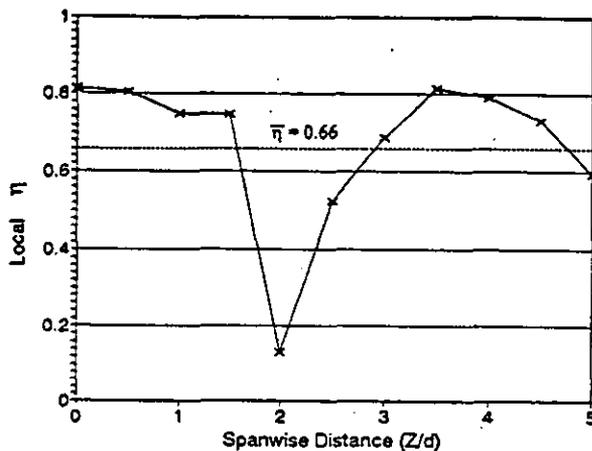
9

Figure 11 : Spanwise η at $x/d=5$ for $M_\infty=0.64$ and $S_R/d=2$.

The present experiments were done at film cooling hole Reynolds numbers above 1000 in order to maintain turbulent flow throughout the region of interest. When two rows of holes are used for film cooling, the Reynolds numbers for the flow out of the front row of holes will drop to very low values, indeed to zero, if the overall mass flow ratio is low. In any case, the Reynolds numbers vary widely, particularly for the first row of holes. This effect adds further complications when both rows are used together.

Data for double row injection plotted as $\overline{\eta}$ at $x/d = 2.5$ (say) against M_∞, has a different form when plotted as $\overline{\eta}$ against M_{JS}. The use of M_∞ in one case and M_{JS} in the other can be reconciled with the relationship between M_{JS}, M_{44}, and M_∞, approximated by $\dfrac{M_{JS}}{M_{44}} = \dfrac{M_\infty^2 - K^2}{M_\infty^2 + K^2}$ where K depends on the hole positions and on R (see Gartshore et al. (1993)). The value of K is about 0.31 for air coolant in this geometry. An illustrative example may be helpful.

Consider the case of $M_\infty = 0.52$ for double row blowing, for which data was reported by Gartshore et al. (1993). The ratio of flow rates M_{JS}/M_{44} was reported as 0.40 for air and 0.15 for CO_2 as coolant. Using the relationship $M_\infty = (M_{JS} + M_{44})/2$, the value of M_{JS} is found to be 0.30 for air and 0.135 for CO_2. The momentum ratio G for the first hole can then be estimated from its definition and the knowledge that C_p at 15° is 0.75, while $R = 1$ for air and 1.5 for CO_2. Values of G are found to be 0.36 for air and 0.049 for CO_2. Notice first that the mass flow from the first hole depends strongly on the density of the coolant, although the overall mass flow ratio M_∞ remains constant. Notice also that G for the

first hole is above the optimum value of $G^*(\approx 0.1)$ for air but below G^* for CO_2. Apparently then, a lower mass flow from the first hole would lead to an improvement in local film cooling using air, whereas a higher mass flow should be used to achieve the highest possible $\overline{\eta}$ with CO_2. Unfortunately, as the value of M_∞ decreases, the value of M_{JS} also decreases sharply and the Reynolds number effects can become important. Salcudean et al. (1994) have demonstrated the extreme sensitivity to Reynolds number of $\overline{\eta}$ values near the first hole for

$M_\infty \lesssim 0.45$. Comparisons between data in this region at slightly different Reynolds numbers do not show consistent trends. This is expected because of the sensitivity of the transition process to very small changes in orientation, free stream turbulence, and Reynolds number, etc. In general, however, the example shows that very low values of M_{JS} are needed to achieve maximum $\overline{\eta}$ just downstream of the front hole. These low values can be estimated from the present value of $G^* \approx 0.1$, the value of C_p at the hole and the value of R.

The use of a spanwise averaged $\overline{\eta}$ is somewhat crude, and disguises the very large spanwise variations which occur in η itself. Figure 11 gives an example of η at $x/d = 5.0$ and $S_R/d = 2.0$ for $M_\infty = 0.64$. The value of $\overline{\eta}$ is 0.66, but η itself varies from 0.16 to 0.8. More complex numerical studies are needed to predict this variation in detail.

For the double row of cooling, the effects of lateral displacement of the first row of holes relative to the second have shown improved spanwise film cooling effectiveness just downstream of the second row. Although the result is not surprising and has been predicted by other authors, it is gratifying to see the extent of the improvement which can be achieved by lateral displacement of a row. Clearly the quantitative results will be affected dramatically by geometry and to a lesser extent by the coolant density. Only air has been used as the coolant in the present double row experiments. For the present spanwise coolant injection of air, an in-line hole arrangement is clearly superior to the more common staggered arrangement, as far as the film cooling effectiveness is concerned.

ACKNOWLEDGMENTS

LIST OF REFERENCES

Eckert, E.R.G., "Analysis of Film Cooling and Full Coverage Film Cooling of Gas Turbine Blades", *ASME J. of Eng. for Gas Turbines and Power*, 106, 206-213 (1984).

Garg, V.K. and Gaugler, R.E., "Heat Transfer in Film Cooled Turbine Blades", ASME 93-GT-81 (1993).

Gartshore, I.S., Salcudean, M., Barnea, Y., Zhang, K., and Aghdasi, F., "Some Effects of Coolant Density on Film Cooling Effectiveness", ASME 93-GT-76 (1993).

Karni, J. and Goldstein, R.J., "Surface Injection Effect on Mass Transfer from a Cylinder in Crossflow: A Simulation of Film Cooling in the Leading Edge Region of a Turbine Blade", *ASME J. of Turbomachinery*, 112, pp. 418-427 (1990).

Leylek, J.H. and Zerkle, R.D., "Discrete-Jet Film Cooling: A Comparison of Computational Results with Experiments", ASME 93-GT-207 (1993).

Luckey, D.W., Winstanley, D.K., Hanus, G.J., and L'Ecuyer, M.R., "Stagnation Region Gas Cooling for Turbine Blade Leading-Edge Applications", *AIAA Journal of Aircraft*, 14, 494-501 (1977).

Mehendale, A.B. and Han, J.C., "Influence of High Mainstream Turbulence on Leading Edge Film Cooling Heat Transfer", *Journal of Turbomachinery*, Vol. 114, pp. 707-715 (1992).

Mick, W.J. and Mayle, R.E., "Stagnation Film Cooling and Heat Transfer Including Its Effects Within the Hole Pattern", *ASME Journal of Turbomachinery*, 110, 66-72 (1988).

Nirmalan, V. and Hilton, L.D., "An Experimental Study of TurbineVane Heat Transfer with Leading Edge and Downstream Film Cooling", *ASME J. of Turbomachinery*, 112, pp. 477-487 (1990).

Ou, S. and Han, J-C., "Unsteady Wake Effect on Film Effectiveness and Heat Transfer Co-efficient from a Turbine Blade with One Row of Air and CO_2 Film Injection", ASME 93-WA/HT-57 (1993).

Pedersen, D.R., Eckert, E.R.G. and Goldstein, R.J., "Film Cooling with Large Density Differences Between the Mainstream and the Secondary Fluid Measured by the Heat-Mass Transfer Analogy", ASME Journal of Heat Transfer 99, pp. 620-627 (1977).

Salcudean, M., Gartshore, I.S., Zhang, K., and McLean, I., "An Experimental Study of Film Cooling Effectiveness Near the Leading Edge of a Turbine Blade", to be published in the *ASME Journal of Turbomachinery* (January 1994 issue).

Zhou, J.-M., Salcudean, M., and Gartshore, I.S., "Prediction of Film Cooling by Discrete-Hole Injection", ASME 93-GT-75 (1993).